AIP Journal of Applied Physics

Transparency pump intensity and differential gain in resonantly pumped W optical pumping injection cavity lasers

L. J. Olafsen and T. C. McAlpine

Citation: Journal of Applied Physics **108**, 053106 (2010); doi: 10.1063/1.3475504
View online: http://dx.doi.org/10.1063/1.3475504
View Table of Contents: http://scitation.aip.org/content/aip/journal/jap/108/5?ver=pdfcov
Published by the AIP Publishing

Transparency pump intensity and differential gain in resonantly pumped W optical pumping injection cavity lasers

L. J. Olafsen[1,a)] and T. C. McAlpine[2]
[1]*Department of Physics, Baylor University, Waco, Texas 76798, USA*
[2]*Department of Physical Sciences, University of Findlay, Findlay, Ohio 45840, USA*

(Received 18 December 2009; accepted 8 July 2010; published online 7 September 2010)

We report the results of a cavity length characterization of a W optical pumping injection cavity (OPIC) laser with a room temperature emission wavelength of 3.2 μm using pump wavelength tuning to achieve resonant optical pumping. Devices with cavity lengths ranging from 312 to 2030 μm are characterized to determine geometry-independent figures of merit. The measurements yield transparency pump intensities I_{tr} that range from 230 W/cm^2 at 100 K to 7.8 kW/cm^2 at 300 K, as gain per unit pump intensity (differential gain) decreases from 0.17 cm/W at 100 K to 0.011 cm/W at 300 K. The characteristic temperature of the transparency pump intensity is 55.6 K, while the gain per unit pump intensity demonstrates an exponential decay with a characteristic temperature of 67.9 K. Compared to other optically pumped type-II W lasers and electrically injected interband cascade lasers, there is less reduction in the differential gain with increasing temperature, consistent with the high temperature operation of these OPIC devices. © *2010 American Institute of Physics*. [doi:10.1063/1.3475504]

I. INTRODUCTION

Developing efficient, ambient-temperature, continuous wave (cw), or high duty cycle laser sources in the mid-infrared, particularly in the 3 to 4 μm spectral range, remains a challenge for laser researchers. Competing technologies to meet this need include quantum cascade lasers (QCLs)[1–4] and both type-I[5,6] and type-II[7,8] antimonide-based semiconductor lasers. QCLs based upon the InGaAs/InAlAs on InP materials system have been demonstrated below 4 μm,[1] but performance at these relatively short wavelengths has been limited by inadequate conduction band offsets. More recent success has been achieved in pulsed mode employing strain compensated InGaAs/AlAsSb/InP QCLs.[2–4] Continuous wave, above room temperature operation has been achieved in type-I interband GaSb-based lasers with wavelengths extending beyond 3 μm out to 3.3 μm[5,6] utilizing high In content in quinary (AlInGaAsSb) barriers. The type-II antimonide W-well laser[9] is a leading candidate to span the 3 to 4 μm region, especially given recent progress in high-temperature and high-power operation of interband cascade lasers (ICLs).[7,8,10–12] While electrically injected lasers are the ultimate goal from the perspective of compact packaging and high wall-plug efficiency, their optically pumped counterparts have reached higher peak output powers[13,14] and maximum operating temperatures.[15–17] Dual-wavelength emission optically pumped lasers have recently been demonstrated with considerable power at both wavelengths,[18–20] and high brightness operation of optically pumped type-II W semiconductor lasers[13,21] demonstrates strong potential for applications to long-range sensing, infrared countermeasures, and free-space optical communications in the mid-infrared.

To further increase maximum operating temperatures and output powers, detailed characterization is required to determine physical parameters critically tied to the performance of the heterostructure, independent of geometric factors or device fabrication. To this end, the Hakki–Paoli method[22–24] and cavity length studies[25,26] have been employed to quantify gain, loss, and efficiency parameters that may be compared across devices. Optically pumped semiconductor lasers provide an excellent test bed for extending the study of gain and loss mechanisms into the room temperature regime. In this work, we present data for transparency pump intensities and gain per unit pump intensity for an optically pumped type-II W laser employing an optical pumping injection cavity at temperatures from 78 to 325 K emitting at 2.9–3.2 μm. These quantities, which are independent of the device geometry, are optical analogs for the transparency current density and gain per unit current density determined from cavity length[25,26] and Hakki–Paoli[23,24] characterizations of electrically injected ICLs.

The antimonide-based W-well consists of a $Ga_{1-x}In_xSb$ hole confining layer sandwiched between two InAs electron confining layers, which are in turn surrounded by $Ga_{1-y}Al_ySb$ barrier layers. The advantages of the W-well design include excellent carrier confinement due to the large band offsets provided by the $Ga_{1-y}Al_ySb$ barriers, variable band gaps that allow the output frequencies to be tuned into the terahertz range, and strong suppression of nonradiative Auger recombination.[27]

Factors that can limit the efficiency of optically pumped W-well lasers include photon decrement, high waveguide losses due to intervalence band absorption, and insufficient absorbance of the pump beam. When the photon decrement is large, most of the energy used to excite carriers in the active region is converted to heat as the electrons nonradiatively relax to energy levels near the quasi-Fermi level. Increasing the pump wavelength reduces this factor.[14] Interva-

a)Electronic mail: linda_olafsen@baylor.edu.

lence band absorption is proportional to the total number of photoexcited carriers. Reducing the number of W-well periods in the active region (and hence the total number of carriers) therefore reduces this loss, although in doing so the absorption of the pump beam for a single pass through the active region also decreases proportionately. To increase pump absorption, the integrated absorber (IA)[13,28] and the optical pumping injection cavity (OPIC)[29] approaches have been employed successfully to increase the absorption in the active region. While high output powers have been achieved using integrated absorbers,[13,14] OPIC lasers have attained higher maximum operating temperatures.[17,29,30] In the W-OPIC design, the W-well active region is centered between distributed Bragg reflectors (DBRs) that serve as mirrors for an etalon cavity whose resonance at the pump wavelength λ_R results in multiple passes through the active region for greater absorption of the pump photons. GaSb spacers on each side of the active region can adjust the path length for a cavity of net optical thickness $2\lambda_R$. Creating this etalon allows strong pump absorbance to be maintained with fewer W-wells and, consequently, less intervalence band absorption for higher power conversion efficiency.[29] An additional benefit of the OPIC configuration is that the high refractive index of the GaSb spacer layers and the low refractive index of the $AlAs_{0.08}Sb_{0.92}$ in the DBRs provide excellent optical confinement of the lasing mode, making the OPIC a very convenient design for edge emitting lasers.[29,30]

Note that as the device temperature increases, the shift in refractive indices and lattice constants of the constituent materials leads to an increase in λ_R. However, one can still resonantly excite at all temperatures by intentionally growing the structure so that λ_R is slightly longer than the fixed pump wavelength, and then pumping at a slight angle from the growth axis to increase the effective layer thicknesses by an adjustable amount (angle tuning).[29] We also demonstrated previously that for diagnostic purposes, and also for cases where no standard pump source is available, an optical parametric oscillator (OPO) provides a convenient means for tuning the pump to any desired wavelength.[17,31] In the present work, an OPO is used to perform a cavity length (L_c) study on a series of W-OPIC lasers. This allows us to experimentally determine the temperature dependences of the transparency pump intensity and gain per unit pump intensity, and also to compare lasers with differing geometric factors.[10,13,15,23,25,26,30,32]

II. EXPERIMENT

The wafer from which the W-OPIC devices were cleaved was grown by molecular beam epitaxy on an *n*-GaSb substrate, as described previously.[17] The strain-compensated active region, which was designed for emission at ≈ 3 μm at room temperature, has ten periods of an InAs/GaSb/InAs/AlSb type-II W-well with thicknesses 21 Å/34 Å/21 Å/40 Å. These are surrounded on both sides by $AlAs_{0.08}Sb_{0.92}$ hole-blocking layers (100 Å) and GaSb spacer layers (5213 Å). DBRs containing alternating layers of $AlAs_{0.08}Sb_{0.92}$ (1758 Å) and GaSb (1451 Å) enclose the active region and spacers. All the above layer thicknesses are nominal. The top DBR (through which the device is optically pumped) has ten periods and the bottom DBR has 18 1/2 periods. The cavity was designed for resonance at 1.85 μm, so the device could be pumped by an available laser diode array. However, the normal incidence reflectance spectrum, as measured at room temperature by a Fourier transform infrared (FTIR) spectrometer, yielded λ_R between 1.79 and 1.83 μm (corresponding to measurements at the wafer's edge or center, respectively).[31] While the 1.85 μm source could not angle tune to the shorter λ_R of this sample, the OPO is suitable for pumping at all of the required wavelengths.

All of the devices employed in the present cavity length study were taken from the same region of the W-OPIC wafer. After the substrate was lapped and polished to a thickness of ≈ 190 μm, several devices were cleaved from a region intermediate between the wafer's edge and center. Five cavities with lengths of 2030, 912, 753, 399, and 310 μm were employed in the study, although the 399 μm laser bar was characterized only at low temperatures ($T \leq 100$ K). To reduce systematic errors, the various cavity lengths were randomized with respect to position on the wafer.

The lasers with uncoated facets were individually mounted on an oxygen-free high conductivity copper heat sink with silver paint to provide good thermal contact. The heat sink was then attached to the cold finger of an Advanced Research Systems Helitran cryostat system to control its temperature. Light-light curves were taken by recording the pulsed output power and wavelength-dependent pump intensity at various temperatures between 78 and 325 K.

Each device was optically pumped at normal incidence, at several wavelengths around the resonance λ_R, to determine the minimum threshold intensity and maximum efficiency. This was accomplished using the wavelength-tunable beam (1740–1800 nm for this work) from an OPO pumped by the third harmonic of a pulsed Nd:yttrium aluminum garnet (YAG) laser. The linewidth of the OPO output, as measured by step-scan FTIR, is ~ 2 nm. The pump pulse of duration ≈ 4 ns was focused in one direction onto the laser's surface to a stripe width of ≈ 200 μm. The overall maximum intensity of the pump beam was controlled by a set of calibrated neutral density filters. The intensity during the experiment was then varied by using an achromatic half-wave retarder to rotate the polarization (initially horizontal) while a broadband polarizing-cube beam-splitter transmitted only the horizontally polarized component of the beam. This generated an attenuated pump beam with horizontal polarization. A cavity type pyroelectric energy probe connected to a dual-channel energy meter measured the portion of the pump pulse energy that was reflected from a calibrated broadband beam-splitter at 45° incidence. The broadband beam-splitter was placed between the broadband polarizing cube beam-splitter and the neutral density filters, since the attenuation of the beam from the filters would have left the energy too small to measure accurately with the energy probe.

The radiation from one edge facet of the OPIC laser was collected through a short focal length calcium fluoride lens that focused the beam onto a photovoltaic InSb detector, whose collection efficiency in the plane of the detector element was taken into account. To prevent the detector from

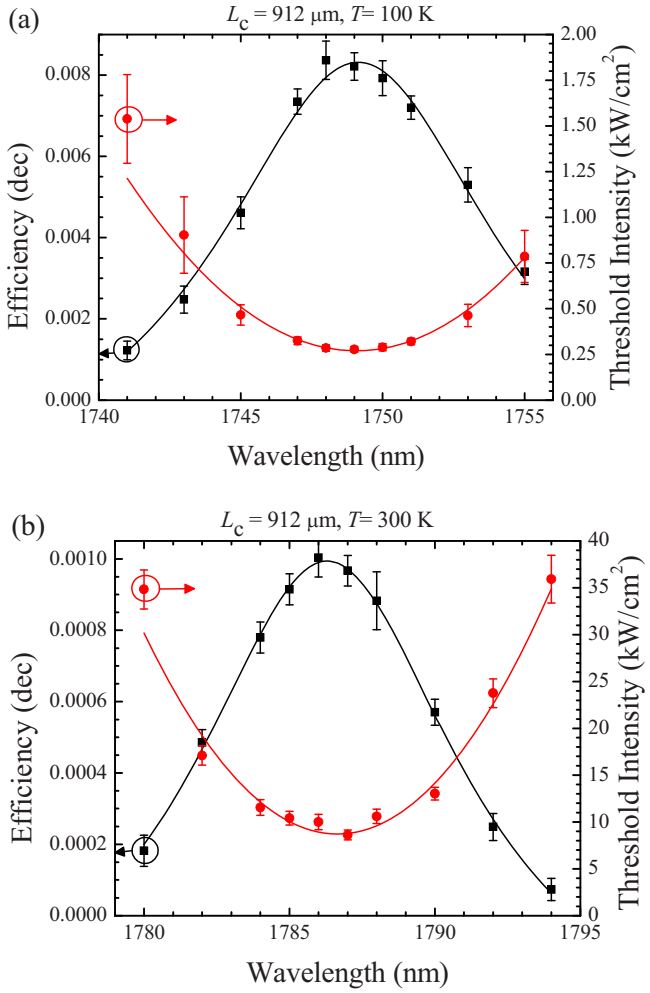

FIG. 1. (Color online) Power conversion efficiency (black squares, left axis) and threshold intensity (red circles, right axis) vs pump wavelength at (a) 100 and (b) 300 K for a cavity length of 912 μm.

saturating, calibrated metallic neutral density filters were used to attenuate the output beam. A long-wave pass filter (cutting off at $\lambda < 2400$ nm) was attached to the front of the InSb detector to block scattered pump radiation. Spectral characterization was performed by diverting the output beam through a monochromating spectrometer.

III. EXPERIMENTAL EFFICIENCIES AND THRESHOLDS

Peak wavelengths for the resonantly pumped OPIC device with 753 μm cavity length increased approximately linearly with temperature, from 2.86 μm at 80 K to 3.20 μm at 325 K, which is representative of all the devices and corresponds to a rate of 1.44 nm/K. That the central wavelength did not display any systematic variation with pump intensity suggests that no significant heating occurred up to the highest pump intensity utilized.

Figure 1 illustrates that consistent lasing thresholds (red circles, right axis) and power conversion efficiencies (black boxes, left axis) are obtained when the pump wavelength is varied at fixed pump location and temperature. The quality of these data for the 912 μm cavity at (a) 100 and (b) 300 K is representative of all the cavity lengths and temperatures studied. The maximum power conversion efficiencies, obtained from the fits to Lorentzian curves, are used to derive the differential quantum efficiencies reported below, and these values are not corrected for the absorbance of the pump beam, which has a maximum value of 17%, as determined from FTIR reflectance spectra.[31] (The absorbance correction *is* included in determining the external differential quantum efficiencies, η_d.) Parabolic fits to the thresholds yield the minimum values along with an independent determination of the resonant pump wavelengths. As in previous studies employing tuned OPO excitation,[17,31] to within experimental error the minimum I_{th} and maximum η_d occur at the same λ_R (which falls in between the integer nanometer OPO wavelength values employed to acquire the data).

IV. CAVITY LENGTH ANALYSIS AND DATA

Using the linear gain approximation,[33] the threshold pump intensity I_{th} varies inversely with cavity length L_c as[34]

$$I_{th} = I_{tr} - \frac{\ln(R)}{G_i L_c}, \tag{1}$$

where I_{tr} is the transparency pump intensity at which a device of infinite cavity length would need to be pumped to reach threshold (analogous to the transparency current density of a diode laser[24,25]), and G_i is the gain per unit pump intensity with units of cm/W (analogous to the gain per unit current density[25] or differential gain[24] in cm/A), and R is the facet reflectivity (two identical uncoated facets are assumed here), which is estimated using

$$R = \left(\frac{n_{wg} - n_{\text{air}}}{n_{wg} + n_{\text{air}}}\right)^2 \approx 0.33. \tag{2}$$

The waveguide is assumed to consist primarily of GaSb and the temperature-dependent refractive index is[35]

$$n_{wg} \approx n_{\text{GaSb}} \approx 3.71(1 + 8.25 \times 10^{-5} T). \tag{3}$$

The transparency pump intensity depends on carrier density at transparency n_{tr} and internal loss α_i

$$I_{tr} = \frac{1}{G_i}\left(\Gamma \frac{dg}{dn} n_{tr} + \alpha_i\right), \tag{4}$$

where $\Gamma dg/dn$ is the modal differential gain.

The external differential quantum efficiency,

$$\eta_d = \frac{2\varepsilon}{(1 - R')} \frac{\lambda_{\text{lase}}}{\lambda_{\text{pump}}}, \tag{5}$$

is determined from the power conversion efficiency ε, the slope of the output intensity versus pump intensity above threshold. The factor of 2 assumes equal output from both facets, whereas the collection is from only one facet in the experiment. The ratio of the emission wavelength λ_{lase} to the optical pumping wavelength λ_{pump} represents the photon decrement. The sample's surface reflectivity R' is $\approx$0.83 based on an interpolation of room temperature reflectivity values at different points on the wafer as determined via FTIR reflectivity measurements.[31] This value is consistent with calculations using multilayer film theory,[36] but is distinct from the facet reflectivity R given by Eq. (2) above.

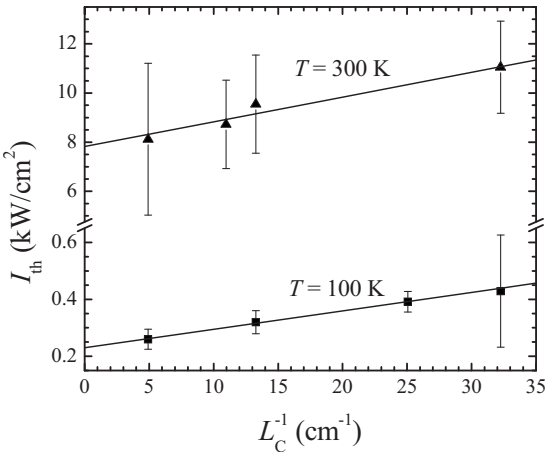

FIG. 2. Threshold pump intensity vs inverse cavity length at 100 K (squares) and 300 K (triangles).

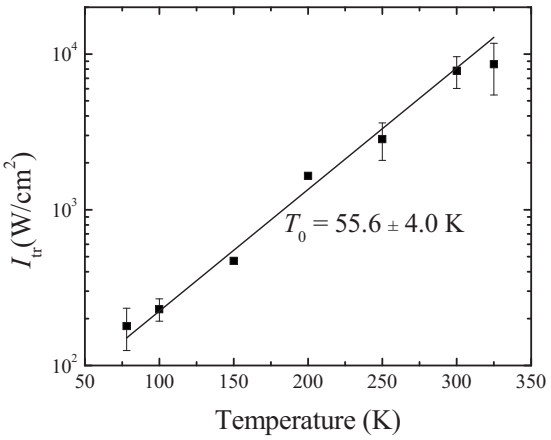

FIG. 3. Transparency pump intensity vs temperature, with a characteristic temperature of 55.6 ± 4.0 K.

The internal quantum efficiency η_i is the probability that the absorption of a pump photon will lead to the generation of a cavity photon, regardless of whether the stimulated emission escapes via a facet. The linear dependence of inverse external differential quantum efficiency on η_i^{-1} and cavity length is[37]

$$\frac{1}{\eta_d} = \frac{1}{\eta_i}\left[1 - \frac{\alpha_i L_c}{\ln(R)}\right], \tag{6}$$

where α_i is the internal loss and R is the facet reflectivity [Eq. (2)]. By measuring I_{th} and η_d for devices of varying cavity length, Eqs. (1) and (6) allow the geometry-independent values of I_{tr}, G_i, η_i, and α_i to be determined by fitting straight lines to I_{th} versus L_c^{-1} and η_d^{-1} versus L_c.

Figure 2 plots threshold pump intensities versus inverse cavity length for the resonantly pumped OPIC lasers operating at 100 and 300 K. These thresholds are seen to vary linearly with inverse cavity length as described in Eq. (1). The intercepts yield transparency pump intensity I_{tr} values of 230 W/cm^2 at 100 K and 7.8 kW/cm^2 at 300 K. While the dependence of threshold intensity on inverse cavity length is approximately linear at 100 and 300 K, at other temperatures experimental fluctuations increase the uncertainties on the extracted transparency intensities.

Figure 3 plots the temperature dependence of the transparency pump intensity I_{tr}, as determined from the intercepts of the linear fits to I_{th} versus L_c^{-1} (see Fig. 2). The transparency pump intensity increases from $I_{tr}=230\pm38$ W/cm^2 at 100 K to 7.82 ± 1.81 kW/cm^2 at 300 K, which corresponds to a transparency characteristic temperature of 55.6 ± 4.0 K. This is consistent with the characteristic temperatures of $T_0 \approx 58.7\pm2.3$ K obtained from fits to $I_{th}=I_0\exp(T/T_0)$ when lasing thresholds for each of the four cavity lengths are measured individually over the full range of temperatures (78–325 K). An earlier OPIC laser, which was cleaved from a region near the center of the same wafer ($L_c=1220$ μm), exhibited a slightly lower characteristic temperature of ≈54 K.[17] The first W-OPIC device ever characterized[29] had an active region with ten periods that emitted at 3.4 μm with characteristic temperature $T_0 \approx 64$ K, slightly higher than the W-OPIC studied in this work. Another early W-OPIC[30] with ten periods emitting at ≈3.7 μm had a lower characteristic temperature of 44 K for a cavity length ≈0.5 mm. The OPIC devices in the present work consistently yielded $T_0 \approx 60$ K, which is comparable with the best values demonstrated in type-II W lasers. Optically pumped lasers enjoy the advantage that they are typically broad area devices that are not etched and consequently do not present regions that introduce additional surface recombination or sidewall losses that can lead to higher thresholds and lower characteristic temperatures.[25]

Gain per unit pump intensity, as determined from linear fits of Eq. (1) at each temperature, is plotted versus temperature in Fig. 4. The values of G_i are seen to range from 0.17 cm/W at 100 K to 0.011 cm/W at 300 K. As is the case for the analogous quantity in electrically driven diode lasers,[24,25] G_i decays exponentially, plotted here with a characteristic temperature of 67.9 ± 16.1 K that fits well the 78–300 K range. The factor of 16 decrease in optical differential gain is an improvement relative to the values determined over the same temperature range for interband cascade lasers in Refs. 24 and 25. In Ref. 24, an ICL emitting at approximately the same wavelengths as the W-OPIC in this work demonstrated a sharper gain reduction of 35 from 78–270 K (≈16 over 100–270 K; the value of 130 K reported in this paper for the

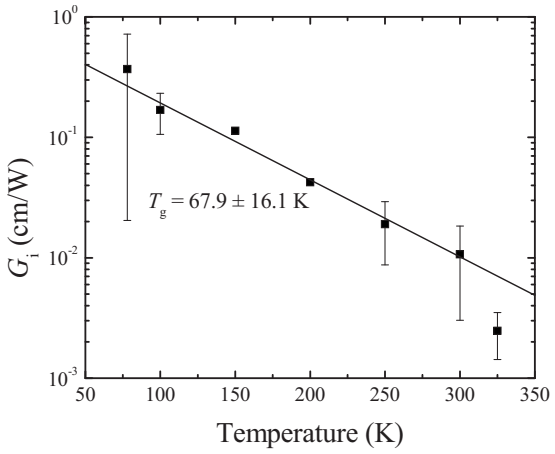

FIG. 4. Gain per unit pump intensity vs temperature. The values follow an exponential decay with a characteristic temperature of 67.9 ± 16.1 K.

characteristic temperature for differential gain appears inconsistent with the presented data). The gain reduction in Ref. 25 was larger, yielding a characteristic temperature of 39 K, well below the 68 K fit in Fig. 4. A more direct comparison to optically pumped lasers may be made considering the type-II W lasers in Ref. 38 that utilized integrated absorber regions for enhanced absorption of the pump beam. Both the W-OPIC and the W-IA yielded comparable values of differential gain at 78 K. The W-IA devices operated to only 130 K, and showed a rapid fall-off of both peak gain and differential gain. The differential gain was measured for a single device and hence had units of gain per pump power rather than gain per pump intensity, but rescaling for the reported pump area, the differential gain per pump intensity decreased from ≈0.14 cm/W at 78 K to ≈0.017 cm/W at 120 K, a significantly more rapid decline than observed in the present work. Based upon gain calculations using the superlattice empirical pseudopotential model,[39,40] the decline in gain of those devices was attributed to the large differences in the conduction and valence subband curvatures inherent to the W structure. The improved temperature dependence of the differential gain from OPIC lasers presented here, which share the type-II W configuration of the active region, indicate that the difference in subband curvatures likely is not the sole culprit in gain reduction in the integrated absorber structures.

At 78 K, the external differential quantum efficiency at resonance pumping from the laser with $L_c=399$ μm was 20.1%, which is lower than expected. At 300 K, η_d was 1.9% for $L_c=2030$ μm, while at 325 K the device with $L_c=912$ μm yielded the highest external differential quantum efficiency (1.5%) and the 2030 μm cavity had an $\eta_d=1.0\%$. The external differential quantum efficiencies demonstrate an exponential decay, and an average characteristic temperature of 110 ± 1 K. Like Ongstad *et al.*,[38] a rapid decrease in internal efficiency with temperature is observed, but this does not limit high temperature operation of the OPIC in the same manner as for the integrated absorbers. The higher temperature operation may then be attributable to the improved gain per pump intensity (differential gain).

Overall, the η_d values derived from the slope efficiencies are lower than anticipated, which may in part be a result of the relatively low pump beam absorbance. In the earliest OPIC lasers, pump absorbances were determined to be 57%[29] and 71%,[30] while in this work the maximum possible values (determined from FTIR reflectance spectra) are less than 25%, and very likely less than 17% for the portion of the wafer from which these devices were taken. One of the continuing challenges for the OPIC laser is to design a structure with the proper balance of sufficient absorption in the notch of the reflectivity plateau while maintaining high enough reflectivity to ensure multiple passes of the pump beam through the active region of the device.

While the threshold intensity versus L_c^{-1} gave relatively consistent results across the 78–325 K temperature range, the η_d^{-1} versus cavity length data did not yield as regular a picture. For example, while the 100 K threshold data shown in Fig. 2 vary with temperature as anticipated, the short-cavity (<400 μm) results for the inverse efficiency increase, as might be expected when mirror loss dominates in shorter cavities. At 100 K, the best fit determined the internal loss to be 1.3 cm^{-1}, increasing to 6.5 cm^{-1} at 250 K. The variation in internal loss is approximately linear in the 100–300 K range, and a linear fit to these data is shown in Fig. 5. Though these internal loss values appear to be quite low, they are consistent with determinations from a cavity length study of a 3.4 μm integrated absorber type-II W laser.[38] In that work, the authors felt that losses found from Hakki–Paoli measurements of the gain were more reliable due to the potential for substrate modes to affect the measurement of differential quantum efficiencies.[41] With the thick DBR bottom mirror in the present devices, this is not as likely to be the case,[42] but Hakki–Paoli measurements of the OPIC lasers might still be instructive in future work, particularly given some evidence of nonuniformity across the wafer.

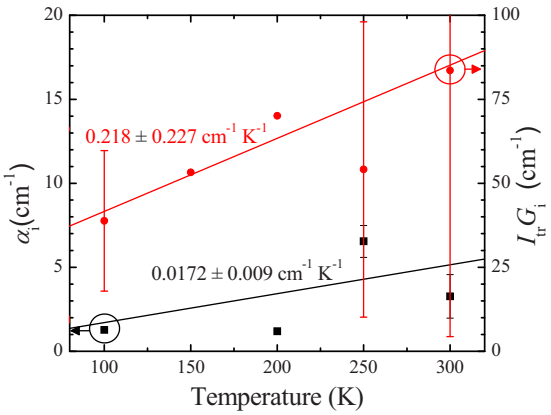

FIG. 5. (Color online) Internal loss (squares, left axis) and the product of the transparency intensity and differential gain (circles, right axis) vs temperature.

Other factors that may influence the calculation of η_d are the Gaussian lateral profile of the pump beam,[26] absorption of the pump beam, or any factors that underestimate the output power from the semiconductor laser. In addition to the photon decrement, pump surface reflectivity, and emission from two facets included in Eq. (5), the power conversion (slope, ε) efficiency was corrected for the collection efficiency. It was assumed that due to the high reflectivity of the 18 1/2-period mirror between the active region and the substrate that any of the pump beam not reflected from the surface was absorbed, and this also could lead to an underestimate of η_d. The pump reflectivity factor is based on room temperature FTIR spectra on another part of the wafer and here assumed to be constant with temperature.

The product of the transparency intensity and the gain per unit pump intensity (circles, right axis) is also shown in Fig. 5. This quantity is equivalent to $\Gamma(dg/dn)n_{tr}+\alpha_i$ [cf., Eq. (4)], where the first term is a product of the modal gain and the transparency carrier density, and the second term is the internal loss. In the most extreme case, in which internal loss completely dominates, these values would provide an upper bound for the internal loss in these lasers, which is approximately 39 cm^{-1} at 100 K and 85 cm^{-1} at 300 K. However, even with the decrease in modal gain with increasing temperature, the internal loss should not completely dominate as the transparency carrier density increases with

increasing temperature. The $I_{tr}G_i$ product provides a useful limit for temperatures up through 300 K; at 325 K the threshold intensity and gain per pump intensity appear to fall below the characteristic temperature trend and thus provide a less reliable bound.

V. CONCLUSIONS

A cavity length study of a W-OPIC laser has yielded transparency intensities and gain per unit pump intensities at temperatures ranging from 78 to 325 K. Transparency pump intensities increase from 230 W/cm^2 at 100 K to 7.8 kW/cm^2 at 300 K, and gain per unit pump intensity decreases from 0.17 to 0.011 cm/W across the same temperature range. The characteristic temperature, both for the threshold intensities of individual devices and for the extrapolated transparency pump intensity, is comparable to the highest values for type-II W lasers (~60 K). In addition, these lasers demonstrate improved differential gain reduction with increasing temperature relative to interband cascade lasers and optically pumped laser employing an integrated absorber. The above-room-temperature operation of these devices may be attributed to the combination of relatively high characteristic temperature and comparatively slow decrease in differential gain with increasing temperature.

ACKNOWLEDGMENTS

This research was supported by The Office of Naval Research (Grant No. N00014-01-1-0567), The Air Force Office of Scientific Research (Grant No. FA9550-04-1-0433), and by the University of Kansas General Research Fund. The authors gratefully acknowledge W. W. Bewley, J. R. Meyer, and I. Vurgaftman from Naval Research Laboratory for sample design and extensive discussions and H. Lee and R. U. Martinelli, formerly of Sarnoff Corporation, for sample growth. Thanks also to K. G. Young and M. R. Santilli for their assistance in the laboratory.

[1]J. Faist, F. Capasso, D. L. Sivco, A. L. Hutchinson, S. G. Chu, and A. Y. Cho, Appl. Phys. Lett. **72**, 680 (1998).
[2]Q. Yang, C. Manz, W. Bronner, N. Lehmann, F. Fuchs, K. Köhler, and J. Wagner, Appl. Phys. Lett. **90**, 121134 (2007).
[3]S. Y. Zhang, D. G. Revin, J. W. Cockburn, K. Kennedy, A. B. Krysa, and M. Hopkinson, Appl. Phys. Lett. **94**, 031106 (2009).
[4]S. Y. Zhang, D. G. Revin, J. P. Commin, K. Kennedy, A. B. Krysa, and J. W. Cockburn, Electron. Lett. **46**, 439 (2010).
[5]G. Belenky, L. Shterengas, D. Wang, G. Kipshidze, and L. Vorobjev, Semicond. Sci. Technol. **24**, 115013 (2009).
[6]T. Hosoda, G. Kipshidze, G. Tsvid, L. Shterengas, and G. Belenky, IEEE Photon. Technol. Lett. **22**, 718 (2010).
[7]C. S. Kim, M. Kim, W. W. Bewley, J. R. Lindle, C. L. Canedy, J. Abell, I. Vurgaftman, and J. R. Meyer, Appl. Phys. Lett. **95**, 231103 (2009).
[8]I. Vurgaftman, C. L. Canedy, C. S. Kim, M. Kim, W. W. Bewley, J. R. Lindle, J. Abell, and J. R. Meyer, New J. Phys. **11**, 125015 (2009).
[9]J. R. Meyer, C. A. Hoffman, F. J. Bartoli, and L. R. Ram-Mohan, Appl. Phys. Lett. **67**, 757 (1995).
[10]C. L. Canedy, W. W. Bewley, J. R. Lindle, C. S. Kim, M. Kim, I. Vurgaftman, and J. R. Meyer, J. Electron. Mater. **35**, 453 (2006).
[11]K. Mansour, Y. Qiu, C. J. Hill, A. Soibel, and R. Q. Yang, Electron. Lett. **42**, 1034 (2006).
[12]M. Kim, C. L. Canedy, W. W. Bewley, C. S. Kim, J. R. Lindle, J. Abell, I. Vurgaftman, and J. R. Meyer, Appl. Phys. Lett. **92**, 191110 (2008).
[13]A. P. Ongstad, R. Kaspi, G. C. Dente, M. L. Tilton, and J. Chavez, Appl. Phys. Lett. **90**, 191107 (2007).
[14]R. Kaspi, A. P. Ongstad, G. C. Dente, J. R. Chavez, M. L. Tilton, and D. M. Gianardi, Appl. Phys. Lett. **88**, 041122 (2006).
[15]W. W. Bewley, C. L. Felix, E. H. Aifer, I. Vurgaftman, L. J. Olafsen, J. R. Meyer, H. Lee, R. U. Martinelli, J. C. Connolly, A. R. Sugg, G. H. Olsen, M. J. Yang, B. R. Bennett, and B. V. Shanabrook, Appl. Phys. Lett. **73**, 3833 (1998).
[16]W. W. Bewley, C. L. Felix, I. Vurgaftman, D. W. Stokes, E. H. Aifer, L. J. Olafsen, J. R. Meyer, M. J. Yang, B. V. Shanabrook, H. Lee, R. U. Martinelli, and A. R. Sugg, Appl. Phys. Lett. **74**, 1075 (1999).
[17]T. C. McAlpine, K. R. Greene, M. R. Santilli, L. J. Olafsen, W. W. Bewley, C. L. Felix, I. Vurgaftman, J. R. Meyer, H. Lee, and R. U. Martinelli, J. Appl. Phys. **96**, 4751 (2004).
[18]A. P. Ongstad, R. Kaspi, A. Tauke-Pedretti, J. C. Chavez, M. L. Tilton, and G. C. Dente, Appl. Phys. Lett. **94**, 241111 (2009).
[19]A. Tauke-Pedretti, A. P. Ongstad, M. L. Tilton, J. C. Chavez, and R. Kaspi, IEEE Photon. Technol. Lett. **21**, 1011 (2009).
[20]R. Kaspi, A. P. Ongstad, G. C. Dente, M. L. Tilton, and A. Tauke-Pedretti, IEEE Photon. Technol. Lett. **20**, 1467 (2008).
[21]A. P. Ongstad, G. C. Dente, M. L. Tilton, J. C. Chavez, R. Kaspi, and D. M. Gianardi, *Conference on Lasers and Electro-Optics (CLEO) and the Quantum Electronics and Laser Science Conference (QELS)* (Optical Society of America, Washington, DC, 2010), CTuE6.
[22]B. W. Hakki and T. L. Paoli, J. Appl. Phys. **46**, 1299 (1975).
[23]S. Suchalkin, J. Bruno, R. Tober, D. Westerfeld, M. Kisin, and G. Belenky, Appl. Phys. Lett. **83**, 1500 (2003).
[24]A. Soibel, K. Mansour, Y. Qiu, C. J. Hill, and R. Q. Yang, J. Appl. Phys. **101**, 093104 (2007).
[25]W. W. Bewley, J. R. Lindle, C. L. Canedy, M. Kim, C. S. Kim, D. C. Larrabee, I. Vurgaftman, and J. R. Meyer, J. Appl. Phys. **103**, 013114 (2008).
[26]W. W. Bewley, I. Vurgaftman, C. L. Felix, J. R. Meyer, C.-H. Lin, D. Zhang, S. J. Murry, S. S. Pei, and L. R. Ram-Mohan, J. Appl. Phys. **83**, 2384 (1998).
[27]W. W. Bewley, J. R. Lindle, C. S. Kim, M. Kim, C. L. Canedy, I. Vurgaftman, and J. R. Meyer, Appl. Phys. Lett. **93**, 041118 (2008).
[28]A. P. Ongstad, R. Kaspi, M. L. Tilton, J. R. Chavez, and G. C. Dente, J. Appl. Phys. **98**, 043108 (2005).
[29]C. L. Felix, W. W. Bewley, I. Vurgaftman, L. J. Olafsen, D. W. Stokes, J. R. Meyer, and M. J. Yang, Appl. Phys. Lett. **75**, 2876 (1999).
[30]W. W. Bewley, C. L. Felix, I. Vurgaftman, D. W. Stokes, J. R. Meyer, H. Lee, and R. U. Martinelli, IEEE Photon. Technol. Lett. **12**, 477 (2000).
[31]T. C. McAlpine, K. R. Greene, M. R. Santilli, L. J. Olafsen, W. W. Bewley, C. L. Felix, I. Vurgaftman, J. R. Meyer, M. J. Yang, H. Lee, and R. U. Martinelli, *Progress in Compound Semiconductor Materials III-Electronic and Optoelectronic Applications*, MRS Symposia Proceedings No. 799 (Materials Research Society, Pittsburgh, 2004), p. 211.
[32]D. W. Stokes, L. J. Olafsen, W. W. Bewley, I. Vurgaftman, C. L. Felix, E. H. Aifer, J. R. Meyer, and M. J. Yang, J. Appl. Phys. **86**, 4729 (1999).
[33]W. W. Chow and S. W. Koch, *Semiconductor-Laser Fundamentals: Physics of the Gain Materials* (Springer, Berlin, 1999).
[34]K. S. Mobarhan, *Application Note No. 1: Test and Characterization of Laser Diodes: Determination of Principle Parameters* (Newport, Irvine, 1999).
[35]Ioffe Physico-Technical Institute, Optical properties of Gallium Antimonide (GaSb), http://www.ioffe.rssi.ru/SVA/NSM/Semicond/GaSb/optic.html
[36]G. R. Fowles, *Introduction to Modern Optics*, 2nd ed. (Dover, New York, 1989).
[37]H. C. Casey, Jr. and M. B. Panish, *Heterostructure Lasers* (Academic, New York, 1978).
[38]A. P. Ongstad, R. Kaspi, C. E. Moeller, M. L. Tilton, J. R. Chavez, and G. C. Dente, J. Appl. Phys. **95**, 1619 (2004).
[39]G. C. Dente and M. L. Tilton, J. Appl. Phys. **86**, 1420 (1999).
[40]G. C. Dente and M. L. Tilton, Phys. Rev. B **66**, 165307 (2002).
[41]M. L. Tilton, G. C. Dente, A. P. Ongstad, R. Kaspi, J. Chavez, and D. Gianardi, Fifth International Conference on Mid-IR Optoelectronic Materials and Devices (MIOMD-V), Annapolis, MD, 2002, p. 165.
[42]W. W. Bewley, C. L. Canedy, C. S. Kim, I. Vurgaftman, M. Kim, and J. R. Meyer, Physica E (Amsterdam) **20**, 466 (2004).